Scaling Approach for Sub-Kilowatt Hall-Effect Thrusters

Eunkwang Lee,* Younho Kim,† and Hodong Lee‡
Satrec Initiative, Daejeon 34054, Republic of Korea
and
Holak Kim,§ Guentae Doh,¶ Dongho Lee,** and Wonho Choe††
Korea Advanced Institute of Science and Technology, Daejeon 34141, Republic of Korea

DOI: 10.2514/1.B37424

Properly determining the size and predicting the performance of a Hall-effect thruster (HET) is an essential process in the early phase of thruster design. In this paper, the scaling relations for a sub-kilowatt HET were derived in the form of linear equations from the physical relationships and the approaches found in previous studies. Because the anode power and voltage are major constraints in thruster design, the equations were given as a function of those parameters. The linear coefficients in the proposed scaling equations were determined from linear regression analysis on the test data from low-power HETs that consume less than 1.35 kW. A large discrepancy was shown between the coefficients and the values obtained from test results from a wide power range due to the losses in small thrusters. A low-power HET that consumes 360 W and applies 300 V at the anode was designed on the basis of the proposed relationship. To validate the thruster design using the proposed relations, the thruster was tested and the results showed that the measured thrust fell within the 95% prediction band.

Nomenclature

A_c	=	channel cross-sectional area, m^2
$C_{\dot{m}}$	=	proportionality constant for the anode mass flow rate
C_p	=	proportionality constant for the anode power
d	=	channel mean diameter, m
e	=	elementary electric charge, C
h	=	channel width, m
I_d	=	discharge current, A
I_i	=	ion current, A
$I_{\mathrm{sps},a}$	=	anode specific impulse, s
L	=	channel length, m
m_a	=	propellant atom mass, kg
$\dot{m}_a$	=	anode mass flow rate, kg/s
m_i	=	Ion mass, kg
$\dot{m}_i$	=	ion mass flow rate, kg/s
n_a	=	propellant particle number density, m^{-3}
P_d	=	anode power, W
T	=	thrust, N
U_d	=	anode voltage, V
U_{loss}	=	potential losses, V
v_a	=	propellant atom velocity, m/s
v_i	=	ion velocity, m/s
α	=	ionized propellant mass fraction
θ_d	=	beam divergence correction factor
ρ_a	=	propellant atom density, kg/m^3

Received 23 October 2018; revision received 6 June 2019; accepted for publication 7 June 2019; published online 24 July 2019.

*Associate Research Engineer, Propulsion Engineering, R&D Center; eklee.space@gmail.com. Member AIAA.

†Senior Research Engineer, Propulsion Engineering, R&D Center; yhk@satreci.com. Member AIAA.

‡Associate Research Engineer, Propulsion Engineering, R&D Center; hdlee@satreci.com. Member AIAA.

§Postdoctoral Researcher, Department of Physics; holak_phys@kaist.ac.kr.

¶Graduate Student, Department of Physics; kuntae21@kaist.ac.kr.

**Graduate Student, Department of Physics; dhlee.phys@kaist.ac.kr.

††Professor, Department of Nuclear and Quantum Engineering; wchoe@kaist.ac.kr. Member AIAA.

I. Introduction

THE application of small satellites has become more diverse as miniaturized satellite payloads have enabled various services, including remote sensing and telecommunications, with a small satellite platform [1–3]. The various types of satellite missions and the advent of new concepts, such as satellite formation flying, place a great importance on the propulsion system because they require accurate satellite position control [3]. A Hall-effect thruster (HET) is a propulsive device that generates thrust by expelling an ionized propellant, and it is an attractive thruster option for a satellite that requires a large velocity change, or ΔV, due to its high specific impulse, thrust efficiency, and power-to-thrust ratio [4].

The majority of HETs have been flown with relatively large satellites in geostationary orbits that require relatively large ΔV, and most of the satellites have carried thrusters that consume more than 1 kW [5]. However, as the applications for small satellites increase, the required ΔV has also increased to aid in the satellites' maneuverability, such as in very low-Earth-orbit operations and orbit controls for forming constellations. As a result, the demand for low-power HETs, which consume power in the sub-kilowatt range, is rapidly increasing [6–8].

Unlike other types of thrusters, such as chemical thrusters, there is no analytic solution for sizing the thruster and predicting its performance due to the nonlinear and complicated physics involved in the plasma interaction such as anomalous electron transport and electron-wall interaction [9]. In designing HETs, having a scaling relation would be helpful because it could reduce the effort required to optimize the thruster; therefore, to design low-power HETs, it is important to find a scaling relation. Extensive numerical and experimental studies have been conducted to derive scaling relations and to predict the performance of HETs [10–20]. However, numerical approaches based on physical modeling usually provide results that deviate from the experimental data because of the assumptions such approaches make [10]. Furthermore, some of the numerical approaches still require empirical coefficients to ensure their accuracy [11,12]; thus, the studies may not be practical for designers without a test database. For these reasons, a scaling relation on the basis of empirical data is developed in the present work.

Scaling laws extracted from the experimental data cover a wide range of power and thrust levels [13–15]; however, their relations may be too general to be used for designing a sub-kilowatt HET because they apply to thrusters operating at power levels up to several kilowatts. The predicted performance from published empirical scaling laws may not agree well with the actual performance within the sub-kilowatt range because of losses coming from the large surface-to-volume ratio in small HETs [6,20]. Although Daren et al.

Table 1 Collected data set for the low-power (< 1.35 kW) Hall-effect thrusters

Thruster	P, W	U_d, V	d, mm	h, mm	L, mm	$\dot{m}_a$, mg/s	T, mN	$I_{sps,a}$, s
SPT-20 [21]	52.4	180	15.0	5.0	32.0	0.47	3.9	839
SPT-25 [22]	134	180	20.0	5.0	N/A	0.59	5.5	948
HET-100 [23]	174	300	23.5	5.5	14.5	0.50	6.8	1386
KHT-40 [24]	187	325	31.0	9.0	25.5	0.69	10.3	1519
KHT-50 [24]	193	250	42.0	8.0	25.0	0.88	11.6	1339
HEPS-200	195	250	42.5	8.5	25.0	0.88	11.2	1300
BHT-200 [25,26]	200	250	21.0	5.6	N/A	0.94	12.8	1390
KM-32 [27]	215	250	32.0	7.0	16.0	1.00	12.2	1244
SPT-50M [28]	245	200	39.0	11.0	25.0	1.50	16.0	1088
SPT-30 [23]	258	250	24.0	6.0	11.0	0.98	13.2	1234
KM-37 [29]	283	292	37.0	9.0	17.5	1.15	18.5	1640
CAM200 [30,31]	304	275	43.0	12.0	N/A	1.09	17.3	1587
SPT-50 [21]	317	300	39.0	11.0	25.0	1.18	17.5	1746
A-3 [21]	324	300	47.0	13.0	30.0	1.18	18.0	1821
HEPS-500	482	300	49.5	15.5	25.0	1.67	25.9	1587
BHT-600 [26,32]	615	300	56.0	16.0	N/A	2.60	39.1	1530
SPT-70 [33]	660	300	56.0	14.0	25.0	2.56	40.0	1593
SPT-100 [9,34]	1350	300	85.0	15.0	25.0	5.14	81.6	1540

N/A, not available.

[19] improved the existing scaling law by extending the low-power regime down to 1.35 kW, their work was based on the limited data from only four stationary plasma thrusters. Moreover, as some studies did not explicitly provide specific correlations or coefficients for their scaling laws, readers manually extrapolated the data from the given figures [13–15].

Accordingly, the present study mainly aims to narrow down the power range of the scaling laws based on the existing scaling relations introduced by Dannenmayer and Mazouffre [13] and Shagayda [15]; thus, the experimental data within the power range up to 1.35 kW were used to improve the scaling law for the sub-kilowatt Hall thruster design. In this paper, we refer to low-power HETs as those thrusters that consume less than 1.35 kW for the sake of consistency with the collected data. To characterize the thruster geometry and performance in the nominal operating condition, the following values were extracted: anode power (P_d), anode voltage (U_d), channel mean diameter (d), channel width (h), channel length (L), anode mass flow rate ($\dot{m}_a$), thrust (T), and anode specific impulse ($I_{sps,a}$). The collected data set of thrusters is listed in Table 1, and most data were obtained under the background pressure less than 3.0×10^{-3} Pa corrected for xenon. All the thrusters discussed herein are annular-type Hall thrusters, which use xenon as a propellant. Based on the data analysis, the explicit scaling relations for low-power HETs were obtained. Finally, a thruster was designed by using the proposed relationships and its design validity was evaluated by comparing its experiment result with the predicted values from the proposed relations.

II. Revisiting and Verifying the Existing Scaling Laws with Empirical Data

In the early stage of HET design, it is important to properly determine the thruster geometry and predict the thruster performance because it reduces the effort required to optimize the thruster. Therefore, the collected thruster data in the sub-kilowatt range were examined for whether they agreed well with the existing scaling laws, and then the relations were improved to be in accordance with the thruster data. The power consumption and the anode voltage are major constraints on thruster design because the available power for thruster operation is usually limited by the available power from a spacecraft and the anode voltage directly affects the power processing module design; thus, the analytic scaling relations were derived as a function of the anode power and voltage.

A. Anode Flow Rate

The fluid mass flow rate, in general, can be calculated by taking a surface integral of the mass flux over a certain area, A_c; thus, the anode mass flow rate $\dot{m}_a$ in the thruster channel is:

$$\dot{m}_a = \iint_A \rho_a \boldsymbol{v_a} \cdot \mathrm{d}\boldsymbol{A_c} \tag{1}$$

where ρ_a is the mass density of the fluid, and v_a is the flow velocity.

When we assume that the propellant flow is uniform and the propellant temperature is fixed throughout the channel, the propellant will have a constant velocity v_a. The equation is then:

$$\dot{m}_a = \rho_a v_a A_c \tag{2}$$

Because annular-type HETs are considered herein, the cross-sectional area A_c can be obtained by multiplying the perimeter of the channel centerline by the channel width h. In addition, the flow density ρ_a is the product of the propellant number density n_a and its particle mass m_a; thus, $\dot{m}_a$ is equal to:

$$\dot{m}_a = \pi n_a m_a v_a h d \tag{3}$$

According to the data plot shown in Fig. 1, the anode flow rate is almost proportional to the product of h and d. This means that the flux of atoms into the thruster should be maintained at a certain level to ensure a stable plasma discharge and an efficient thruster operation. In other words, the number density in low-power thrusters should be constantly maintained. This result is also consistent with the result in Ref. [13]. Thus, Eq. (3) can be written as follows:

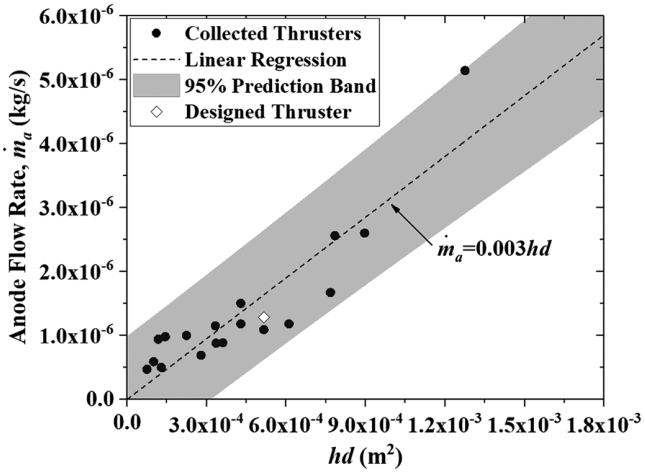

Fig. 1 Anode flow rate variation as a function of hd in low-power (< 1.35 kW) Hall-effect thrusters.

$$\dot{m}_a = C_{\dot{m}} h d \tag{4}$$

The proportionality constant for the anode mass flow rate was obtained by taking the linear regression on the data (Fig. 1). The dashed line represents the linear curve fit. The 95% prediction band (the shaded region) is provided because the linear regression model is not deterministic. The prediction band encompasses all future observations that will fall in the band with 95% probability so that the range between the upper and lower boundaries depends on the deviation of each data point along the curve fit. The relation obtained from the linear regression is as follows:

$$\dot{m}_a\,[\mathrm{kg/s}] = 0.003 h d\,[\mathrm{m}^2] \tag{5}$$

B. Channel Width

The channel width h determines the inner and outer diameters of the annular discharge channel, and it affects the surface-to-volume ratio, which has a strong influence on the thruster performance [6,20]. Several studies have revealed the proportionality between the two dimensional parameters, d and h, based on the wide power range in the thruster data [13,15]. As the thruster size becomes smaller, the thruster requires a stronger magnetic field to confine the electrons properly [20]; for example, HET-100, whose channel width is 5.5 mm, has a maximum magnetic strength of 48 mT at the center of channel exit plane [35], whereas the magnetic strength of SPT-100 thruster with the channel width of 15 mm is about 15 mT [36]. Furthermore, to maintain the similarity in plasma properties such as ion flux, the magnetic strength should be modulated inversely proportional to the channel width [15]. However, room for the magnetic circuit and its supporting structure is physically limited. Therefore, the scaling relation in terms of the channel width h was re-examined in the low-power range.

Figure 2 displays a correlation between d and h in the power range up to 1.35 kW. As can be seen in the figure, h is linearly correlated with d in the narrow range, and the dashed line is a result of the linear regression:

$$h\,[\mathrm{m}] = 0.242 d\,[\mathrm{m}] \tag{6}$$

C. Channel Mean Diameter

The channel mean diameter d should be scaled properly because it determines the overall size of the thruster. In addition, predicting d is important because it is required to calculate the channel width [Eq. (6)] as well as the anode flow rate [Eq. (5)]. Because it was assumed that the anode power and voltage are given numbers, the relation was derived in terms of those parameters.

The anode power P_d is the discharge current I_d times the voltage applied to the anode U_d. The discharge current is a summation of the ion current and the electron current flowing through the anode [37]. If it is assumed that electron transport across the magnetic field is negligible and only a small fraction of multiply charged ions are generated [13,15,38], the discharge current can be written as:

$$I_d \approx I_i \approx \frac{e}{m_a}\dot{m}_i \tag{7}$$

Expressing the ionized propellant fraction as α, the discharge current can be written in terms of $\dot{m}_a$:

$$I_d \approx \frac{e}{m_a}\alpha\dot{m}_a \tag{8}$$

Then, the anode discharge power P_d is:

$$P_d \approx \frac{e}{m_a}\alpha\dot{m}_a U_d \tag{9}$$

where U_d includes the voltage that accelerates ions and the parasitic voltage losses dedicated to the anode sheath and cathode-anode coupling. Substituting Eq. (3) into Eq. (9) yields:

$$P_d \approx \pi e \alpha n_a v_a U_d h d \tag{10}$$

Remembering the proportionality expressed in Eq. (6) and assuming a constant propellant utilization ($\alpha = \mathrm{const}$), we can write the preceding equation as:

$$P_d = C_p U_d d^2 \tag{11}$$

where C_p is the proportionality constant for the discharge power.

Figure 3 illustrates the relation in Eq. (11), and it verifies the linearity between P_d and $U_d d^2$. The linear coefficient C_p was obtained by linearly fitting the data. Although this tendency corresponds to the scaling relation covering a wide power range up to 50 kW proposed by Dannenmayer and Mazouffre [13], the obtained coefficient C_p in Eq. (12) was higher by about 43% compared with the coefficient they provided. The coefficient C_p consists of three major parameters: ionized propellant mass fraction, propellant particle number density, and propellant atom velocity in the channel. In general, low-power HETs have a lower propellant utilization efficiency compared with high-power thrusters [15]; however, the other two parameters may offset the effect of low ionization fraction on the coefficient.

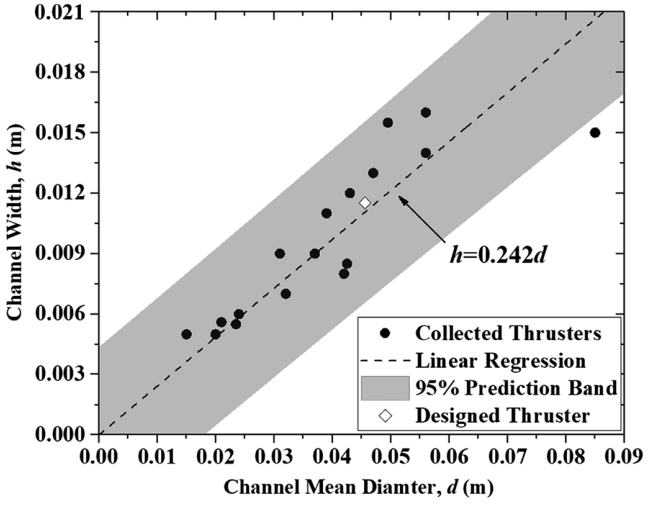

Fig. 2 Channel width variation as a function of channel mean diameter in low-power (< 1.35 kW) Hall-effect thrusters.

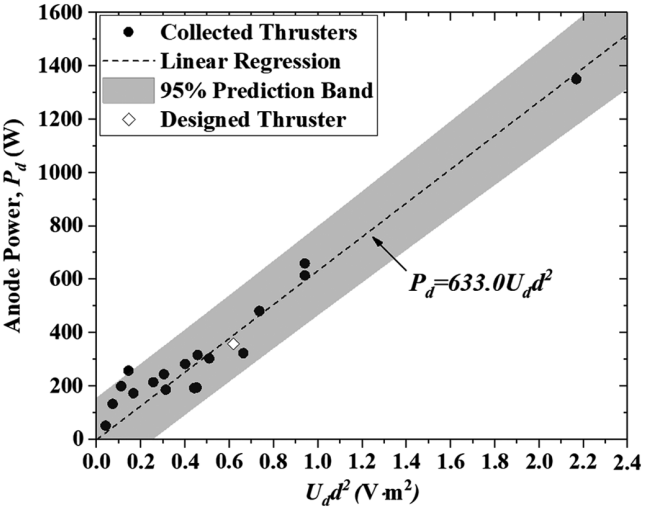

Fig. 3 Relationship between the anode discharge power and the product $U_d d^2$ in low-power (< 1.35 kW) Hall-effect thrusters.

To compare the propellant particle number density in low- and high-power thrusters, the propellant particle number density of thrusters in a power range up to 50 kW was calculated from Eq. (3) with an assumption of a constant propellant velocity. As can be seen in Fig. 4, it was revealed that low-power thrusters that consume less than 1.35 kW have a higher propellant particle number density than the density in high-power HETs. For example, the particle number density of HET-100 thruster listed in Table 1 is about 40% higher than the particle density in P5 thruster, whose anode power is 5 kW [39].

According to Martinez and Walker [40], the mean propellant gas velocity is proportional to the anode temperature. To examine the effect of propellant atom velocity on the coefficient, heat flux through the anode was estimated with a thermal model developed by Mazouffre et al. [41]. According to the analysis, the heat flux through the anode in most low-power thrusters was higher than that in high-power thrusters (see Fig. 5). As the anode in low-power thruster is usually smaller than that in high-power thrusters, it can be supposed that the anode temperature of low-power thrusters would be higher than that of high-power thrusters. In other words, the propellant atom velocity in low-power thrusters is more likely to be higher than that in high-power thrusters. Thus, it can be concluded that the discrepancy in the proportionality constants resulted from the different propellant atom number density and propellant atom velocity in low- and high-power thrusters. Consequently, one can determine the channel diameter for a low-power Hall thruster from Eq. (13).

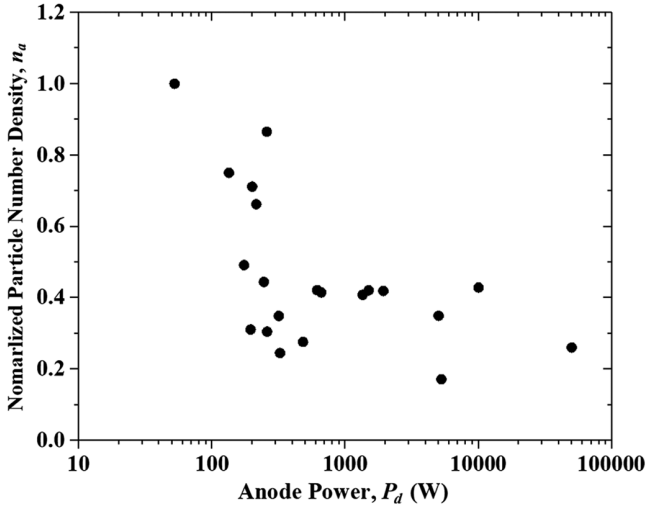

Fig. 4 Normalized particle number density of the thrusters in a power range up to 50 kW.

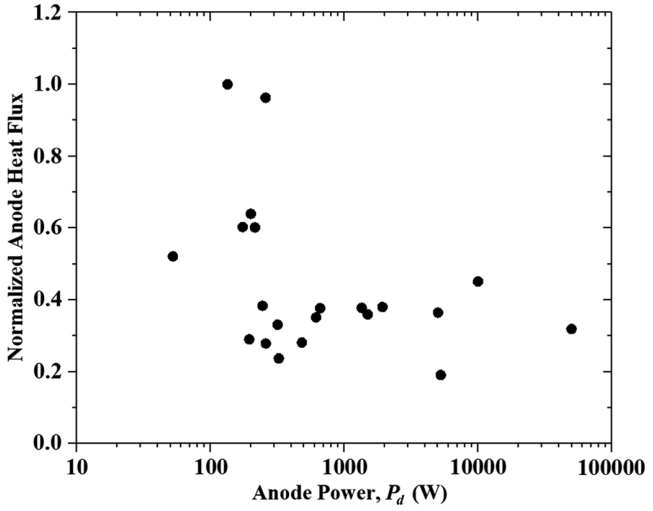

Fig. 5 Normalized anode heat flux of the thrusters in a power range up to 50 kW.

$$P_d\,[\mathrm{W}] = 633.0 U_d d^2\ [\mathrm{V}\cdot\mathrm{m}^2] \tag{12}$$

$$d = \sqrt{\frac{P_d}{633.0 U_d}} \tag{13}$$

D. Thrust

Predicting the thrust is a crucial part in HET scaling because it affects various efficiency factors, such as specific impulse. The thrust is produced by expelling the propellant at high speed. In the case of HETs, the thrust is generated by electrostatically accelerating the ionized propellant through a channel:

$$T = \dot{m}_i v_i = \alpha \dot{m}_a v_i \tag{14}$$

where $\dot{m}_i$ is the ion mass flow rate and v_i is the expelled ion speed. In HETs, the propellant ions spread out when passing the channel exit. By taking the loss caused by the diverged thrust vector of an ion beam into account, the thrust can be given with the divergence factor θ_d, which is the cosine of a beam half-angle:

$$T = \alpha \theta_d \dot{m}_a v_i \tag{15}$$

The ions are accelerated by the electric potential applied at the anode; thus, the ion velocity $v_i$can be described as:

$$v_i = \sqrt{\frac{2e}{m_i}(U_d - U_{\mathrm{loss}})} \tag{16}$$

where U_{loss} represents the electric potential losses in the channel such as a sheath potential drop at the anode and losses due to plasma-wall interaction. Combining Eqs. (15) and (16), one can obtain:

$$T \propto \alpha \theta_d \dot{m}_a \sqrt{U_d - U_{\mathrm{loss}}} \tag{17}$$

Here, if we assume a constant propellant utilization and beam divergence factor, and no potential losses, then the above equation becomes:

$$T \propto \dot{m}_a \sqrt{U_d} \tag{18}$$

As shown in Fig. 6, the thrust linearly increases with $\dot{m}_a\sqrt{U_d}$ for the existing low-power thruster data. The analytic relation extracted from the linear regression result is

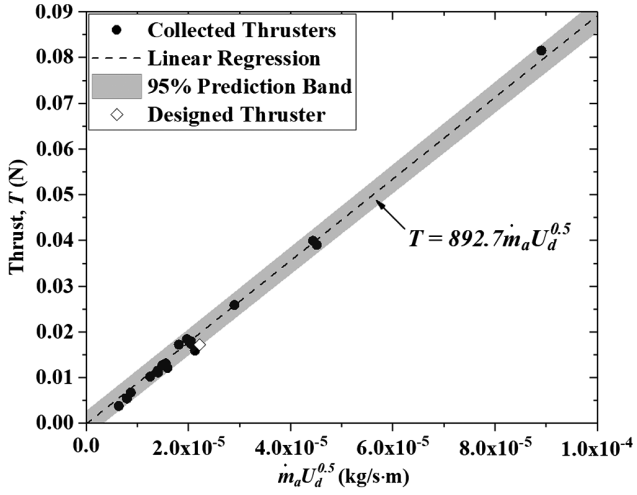

Fig. 6 Relationship between the thrust and the value $\dot{m}_a\sqrt{U_d}$ in low-power (< 1.35 kW) Hall-effect thrusters.

$$T\,[\mathrm{N}] = 892.7\dot{m}_a\sqrt{U_d}\ [\mathrm{kg/(s\cdot V^{0.5})}] \tag{19}$$

A similar approach for a wide power range (< 50 kW) can be found in [13]; however, the proportionality constant obtained is about 17% smaller than the coefficient found in [13]. For simplicity, the above equation was derived based on the assumption of a constant propellant utilization; however, the mass utilization efficiency varies according to the anode voltage and power [15]. To achieve a high thrust efficiency, thruster operation at a high anode voltage is desirable because the propellant utilization efficiency is strongly related to the applied voltage [42]. However, in small and low-power thrusters, the operating anode voltage may be limited because of the thermal constraints, and it deteriorates the mass utilization efficiency. Moreover, a large surface-to-volume ratio in the small thrusters probably resulted in a large potential loss U_{loss} via collisions of ions with the channel wall, and it may lower the voltage utilization efficiency. Hence, the small and low-power thrusters did not effectively generate the thrust, and it resulted in the low proportionality constant. Therefore, the scaling relation acquired from this study [Eq. (19)] will provide a more realistic thrust value for designing a low-power thruster.

III. Experimental Verification of the Proposed Scaling Relations

A. Scaling Procedure

Explicit scaling relations for low-power HETs were derived in the preceding sections. As the power and voltage are user-defined values and the scaling relations are interconnected, the thruster dimensions and performance can be obtained by using the equations provided herein. The channel mean diameter d can be determined from Eq. (13). The channel width h can be obtained by using Eq. (6) and the calculated channel diameter. One can find the required anode flow rate $\dot{m}_a$ from Eq. (5). The thrust T can be predicted with Eq. (19), and other parameters, such as an anode specific impulse $I_{sp,a}$, can be calculated with the obtained values.

Determining the channel length is also important because it is correlated with the acceleration efficiency. As can be seen in Table 1, the channel length L did not show any distinct trends or correlations with other parameters. As the channel length is largely dependent on the magnetic field configuration [43], the optimal channel length may vary with the magnetic field design. In this work, the channel length of 25 mm was used for the initial thruster design.

B. Low-Power Hall-Effect Thruster Design

An engineering model of the HET was designed by following the preceding steps. The thruster was intended to be used in a 400-kg-class satellite platform [44]. The anode power and the voltage were constrained by the system requirements; the values used for the thruster design were 360 W and 300 V, respectively. The scaling result for the 360-W-scale HET and its actual dimensions are presented in Table 2. Figure 7 shows the proposed thruster with a two-cathode configuration. As mentioned in Sec. II.B, to provide a similar plasma condition with other thrusters discussed herein, the maximum magnetic field strength should be scaled inversely proportional to the channel width. Thus, based on the criteria, the magnetic field strength of the designed thruster was set to be about 20 mT at the center of the channel exit. Furthermore, the magnetic configuration was designed to have a peak flux near the channel exit (see Fig. 8). Because of the constraints on the magnetic field strength and topology, it was difficult to make the actual dimensions of the thruster identical to the scaling result; however, as can be seen in Figs. 2 and 3, the actual geometrical parameters stay within the 95% prediction band.

Table 2 Calculated and actual dimensions of a thruster that consumes 360 W of anode power and applies 300 V at the anode

Dimensions	Scaling result	Designed thruster
d, mm	43.4	45.5
h, mm	10.5	11.5
L, mm	— —	25.0

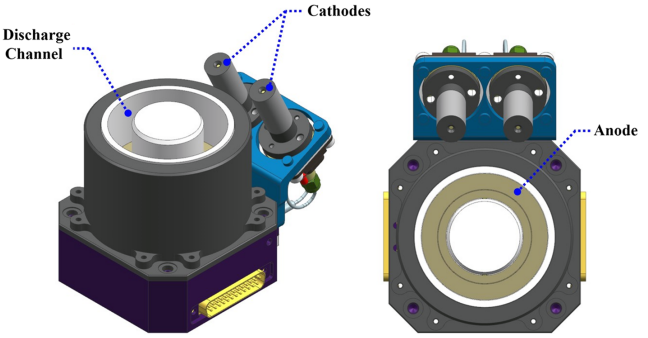

Fig. 7 The low-power Hall-effect thruster design with two cathodes.

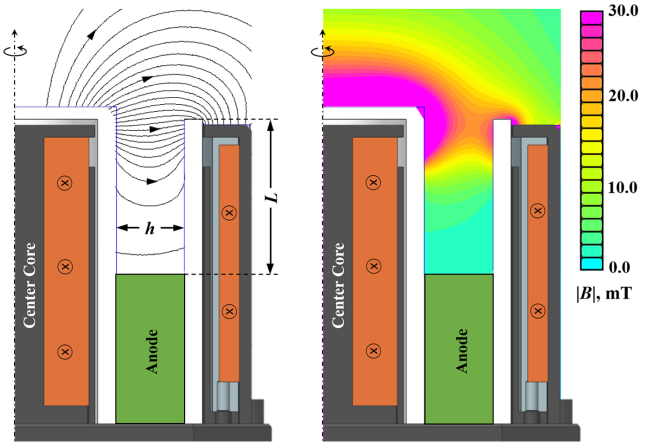

Fig. 8 Magnetic field lines (left) and magnetic flux density contours (right) of the designed Hall-effect thruster.

C. Experiment Results and Discussion

To verify the thruster design and the scaling relations provided herein, the thruster performance was examined. An experiment was conducted in a 3-m-long and 1.5-m-diam vacuum chamber. The chamber is pumped by two cryopumps (ULVAC U22HB) with a nominal pumping speed of 17 $\mathrm{m^3/s}$ on nitrogen or 8 $\mathrm{m^3/s}$ on xenon, and its ultimate pressure is about 9.3×10^{-5} Pa. The chamber background pressure affects the measurement in thrust and efficiency because it is one of the parameters that have an influence on the neutral ingestion effects [45]. The chamber background pressure of 2.7×10^{-3} Pa corrected for xenon was obtained at a continuous xenon flow of 1.28 mg/s, and it was similar to the condition that the referred data obtained. The thruster was placed on a pendulum-type thrust stand, and the thrust was measured by sensing the displacement of the test stand with a combination of a laser and a position-sensitive detector. A commercial hollow cathode (Heatwave HWPES-250) was used in this test to neutralize the expelled ions.

The test result is summarized in Table 3 along with the performance predicted based on scaling relations. Each anode specific impulse was calculated with the predicted and measured

Table 3 Predicted and actual performance of the 360-W-scale Hall-effect thruster

Parameters	Predicted value	Test result
P_d, W	360	357 ± 3
U_d, V	300	300±1
$\dot{m}_a$, mg/s	1.36	1.28±0.01
T, mN	21.1	18.7±0.3
$I_{sp,a}$, s	1579.3	1489.2±61.6

values of flow rate and thrust, respectively. The measured thrust at a comparable anode flow rate is smaller than the predicted value by about 11%. Although the thruster is an engineering model and its parameters that could affect the performance such as magnetic field shape are not optimized, as shown in Fig. 6 and Table 3, the thrust data are closely positioned to the regression data. It can be interpreted that there is room for performance improvement by optimizing the thruster, for example, magnetic field configuration, cathode position, and channel wall material.

IV. Conclusions

In this work, the scaling relations for a low-power (< 1.35 kW) Hall-effect thruster (HET) were reported and the approaches established in the previous research were described. The relations can determine the size and predict performance of the thruster. The correlations described were given as a function of the anode power and voltage because the two parameters are critical constraints when designing a thruster. The linearity of each equation was examined, and the proportional coefficients were explicitly obtained by taking the linear regression on the Hall thruster test data covering a power range up to 1.35 kW. It was revealed that the proportional coefficients obtained with a narrow (up to 1.35 kW) and wide (up to 50 kW) power range showed a large discrepancy, most likely due to the losses in small thrusters. Because the regression models are not deterministic, the 95% prediction bands were provided for flexibility in the thruster design. A low-power HET that consumes 360 W of anode power and 300 V voltage was designed using the proposed scaling approaches, and its design validity was examined through an experimental test. According to the test result, it was confirmed that the thrust generated by the proposed thruster fell within the prediction band. As a result, the scaling relations proposed in this study can be used for the design of a sub-kilowatt-scale Hall thruster. Furthermore, because the coefficients were obtained based on empirical data, the geometrical and performance parameters can be used as the supporting data for numerical simulations.

Acknowledgment

This work was supported by the Space Core Technology Program (Grant No. 2014M1A3A3A02034510) through the National Research Foundation of Korea, funded by the Ministry of Science, Information, Communication Technology, and Future Planning.

References

[1] Sandau, R., "Status and Trends of Small Satellite Missions for Earth Observation," *Acta Astronautica*, Vol. 66, Nos. 1–2, 2010, pp. 1–12. doi:10.1016/j.actaastro.2009.06.008

[2] Selva, D., Golkar, A., Korobova, O., Cruz, I. L., Collopy, P., and de Weck, O. L., "Distributed Earth Satellite Systems: What Is Needed to Move Forward?" *Journal of Aerospace Information Systems*, Vol. 14, No. 8, 2017, pp. 412–438. doi:10.2514/1.I010497

[3] Levchenko, I., Bazaka, K., Ding, Y., Raitses, Y., Mazouffre, S., Henning, T., Klar, P. J., Shinohara, S., Schein, J., Garrigues, L., et al., "Space Micropropulsion Systems for CubeSats and Small Satellites: From Proximate Targets to Furthermost Frontiers," *Applied Physics Reviews*, Vol. 5, No. 1, 2018, Paper 011104. doi:10.1063/1.5007734

[4] Mazouffre, S., "Electric Propulsion for Satellites and Spacecraft: Established Technologies and Novel Approaches," *Plasma Sources Science and Technology*, Vol. 25, No. 3, 2016, Paper 033002. doi:10.1088/0963-0252/25/3/033002

[5] Lev, D., Myers, R. M., Lemmer, K. M., Kolbeck, J., Keidar, M., Koizumi, H., Liang, H., Yu, D., Schonherr, T., del Amo, J. G., et al., "The Technological and Commercial Expansion of Electric Propulsion in the Past 24 Years," *Proceedings of the 35th International Electric Propulsion Conference*, IEPC Paper 2017-242, 2017.

[6] Mazouffre, S., and Grimaud, L., "Characteristics and Performances of a 100-W Hall Thruster for Microspacecraft," *IEEE Transactions on Plasma Science*, Vol. 46, No. 2, 2018, pp. 330–337. doi:10.1109/TPS.2017.2786402

[7] Lev, D. R., Emsellem, G. D., and Hallock, A. K., "The Rise of the Electric Age for Satellite Propulsion," *New Space*, Vol. 5, No. 1, 2017, pp. 4–14. doi:10.1089/space.2016.0020

[8] Pampaloni, A., Trisolini, M., Misuri, T., and Adrenucci, M., "Direct-Drive System Demonstration for a Low-Power Hall Thruster," *Journal of Propulsion and Power*, Vol. 30, No. 4, 2014, pp. 1091–1094. doi:10.2514/1.B35253

[9] Boeuf, J., "Tutorial: Physics and Modeling of Hall Thrusters," *Journal of Applied Physics*, Vol. 121, No. 1, 2017, Paper 011101. doi:10.1063/1.4972269

[10] Garrigues, L., Boyd, I. D., and Boeuf, J. P., "Computation of Hall Thruster Performance," *Journal of Propulsion and Power*, Vol. 17, No. 4, 2001, pp. 772–779. doi:10.2514/2.5832

[11] Kwon, K., Walker, M. L. R., and Mavris, D. N., "Self-Consistent, One-Dimensional Analysis of the Hall Effect Thruster," *Plasma Sources Science and Technology*, Vol. 20, No. 4, 2011, Paper 045021. doi:10.1088/0963-0252/20/4/045021

[12] Mikellides, I. G., Katz, I., Hofer, R. R., and Goebel, D. M., "Magnetic Shielding of a Laboratory Hall Thruster. I. Theory and Validation," *Journal of Applied Physics*, Vol. 115, No. 4, 2014, Paper 043303. doi:10.1063/1.4862313

[13] Dannenmayer, K., and Mazouffre, S., "Elementary Scaling Relations for Hall Effect Thrusters," *Journal of Propulsion and Power*, Vol. 27, No. 1, 2011, pp. 236–245. doi:10.2514/1.48382

[14] Shagayda, A. A., and Gorshkov, O. A., "Hall-Thruster Scaling Laws," *Journal of Propulsion and Power*, Vol. 29, No. 2, 2013, pp. 466–474. doi:10.2514/1.B34650

[15] Shagayda, A. A., "On Scaling of Hall Effect Thrusters," *IEEE Transactions on Plasma Science*, Vol. 43, No. 1, 2015, pp. 12–28. doi:10.1109/TPS.2014.2315851

[16] Kwon, K., Lantoine, G., Russell, R. P., and Mavris, D. N., "A Study on Simultaneous Design of a Hall Effect Thruster and Its Low-Thrust Trajectory," *Acta Astronautica*, Vol. 119, Feb.–March 2016, pp. 34–47. doi:10.1016/j.actaastro.2015.11.002

[17] Kim, V., "Main Physical Features and Processes Determining the Performance of Stationary Plasma Thruster," *Journal of Propulsion and Power*, Vol. 14, No. 5, 1998, pp. 736–743. doi:10.2514/2.5335

[18] Smirnov, A., Raitses, Y., and Fisch, N. J., "Parametric Investigation of Miniaturized Cylindrical and Annular Hall Thrusters," *Journal of Applied Physics*, Vol. 92, No. 10, 2002, pp. 5673–5679. doi:10.1063/1.1515106

[19] Daren, Y., Yongjie, D., and Zhi, Z., "Improvement on the Scaling Theory of the Stationary Plasma Thruster," *Journal of Propulsion and Power*, Vol. 21, No. 1, 2005, pp. 139–143. doi:10.2514/1.5901

[20] Khyms, V., and Martinez-Sanchez, M., "Fifty-Watt Hall Thruster for Microsatellites," *Micropropulsion for Small Spacecraft*, edited by M. M. Micci, and A. D. Ketsdever, Vol. 187, Progress in Astronautics and Aeronautics, AIAA, Reston, VA, 2000, pp. 233–254.

[21] Guerrini, G., Michaut, C., Dudeck, M., and Bacal, M., "Parameter Analysis of Three Small Ion Thruster," *Proceedings of the 2nd European Spacecraft Propulsion Conference*, ESA SP-398, Noordwijk, The Netherlands, 1997, pp. 441–446.

[22] Arkhipov, B., Kim, V., Kozlov, V., Koryakin, A., Murashko, V., Nesterenko, A., Skrylnikov, A., and Lawrence, T., "Small SPT Unit Development and Test," *Proceedings of the 3rd International Conference on Spacecraft Propulsion*, ESA SP-465, Cannes, France, 2000, pp. 399–401.

[23] Misuri, T., and Andrenucci, M., "HET Scaling Methodology: Improvement and Assessment," *Proceedings of the 44th AIAA/ASME/SAE/ASS Joint Propulsion Conference & Exhibit*, AIAA Paper 2008-4806, 2008, doi:10.2514/6.2008-4806

[24] Seo, M., "Comparison of the Low Power Hall Plasma Thruster Performance According to the Geometrical Structure of Discharge Region," Ph.D. Dissertation, Dept. of Physics, KAIST, Daejeon, Republic of Korea, 2013.

[25] Beal, B. E., Gallimore, A. D., Haas, J. M., and Hargus, W. A., Jr., "Plasma Properties in the Plume of a Hall Thruster Cluster," *Journal of Propulsion and Power*, Vol. 20, No. 6, 2004, pp. 985–991. doi:10.2514/1.3765.

[26] Cheng, S. Y., and Martinez-Sanchez, M., "Hybrid Particle-in-Cell Erosion Modeling of Two Hall Thrusters," *Journal of Propulsion and Power*, Vol. 24, No. 5, 2008, pp. 987–998. doi:10.2514/1.36179

[27] Belikov, M. B., Gorshkov, O. A., Dyshlyuk, E. N., Lovtzov, A. S., and Shagayda, A. A., "Development of Low-Power Hall Thruster with

Lifetime up to 3000 Hours," *Proceedings of the 30th International Electric Propulsion Conference*, IEPC Paper 2007-129, Florence, Italy, 2007.

[28] Potapenko, M. Y., and Gopanchuk, V. V., "Characteristic Relationship Between Dimensions and Parameters of a Hybrid Plasma Thruster," *Proceedings of the 32nd International Electric Propulsion Conference*, IEPC Paper 2011-042, Wiesbaden, Germany, 2011.

[29] Belikov, M. B., Gorshkov, O. A., Muravlev, V. A., Rizakhanov, R. N., Shagayda, A. A., and Shnirev, A. U., "High-Performance Low Power Hall Thruster," *Proceedings of the 37th AIAA/ASME/SAE/ASEE Joint Propulsion Conference and Exhibit*, AIAA Paper 2001-3780, 2001, doi:10.2514/6.2001-3780

[30] Lev, D., Eytan, R., Alon, G., Warshavsky, A., Appel, L., Kapulkin, A., and Rubanovych, M., "The Development of CAM200—Low Power Hall Thruster," *Transactions of the Japan Society for Aeronautical and Space Sciences Aerospace Technology Japan*, Vol. 14, No. 30, pp. 217–223. doi:10.2322/tastj.14.Pb_217

[31] Kronhaus, I., Kapulkin, A., Balabanov, V., Rubanovich, M., Guelman, M., and Natan, B., "Discharge Characterization of the Coaxial Magnetoisolated Longitudinal Anode Hall Thruster," *Journal of Propulsion and Power*, Vol. 29, No. 4, 2013, pp. 938–949. doi:10.2514/1.B34754

[32] Lobbia, R. B., and Gallimore, A. D., "Evaluation and Active Control of Clustered Hall Thruster Discharge Oscillations," *Proceedings of the 41st AIAA/ASME/SAE/ASEE Joint Propulsion Conference*, AIAA Paper 2005-3679, 2005, doi:10.2514/6.2005-3679

[33] Hofer, R. R., and Jankovsky, R. S., "A Hall Thruster Performance Model Incorporating the Effects of a Multiply-Charged Plasma," *Proceedings of the 37th AIAA/ASME/SAE/ASEE Joint Propulsion Conference & Exhibit*, AIAA Paper 2001-3322, 2001. doi:10.2514/6.2001-3322

[34] Sankovic, J. M., Hamley, J. A., and Haag, T. W., "Performance Evaluation of the Russian SPT-100 Thruster at NASA LeRC," *Proceedings of the 23rd International Electric Propulsion Conference*, IEPC Paper 93-094, Seattle, WA, 1993, pp. 855–882.

[35] Andrenucci, M., Breti, M., Biagioni, L., Cesari, U., and Saverdi, M., "Characteristics of the XHT-100 Low Power Hall Thruster Prototype," *Proceedings of the 4th International Spacecraft Propulsion Conference*, ESA SP-555, Cagliari, Italy, 2004.

[36] Dannenmayer, K., and Mazouffre, S., "Sizing of Hall Effect Thrusters with Input Power and Thrust Level: An Empirical Approach," *Journal of Technical Physics*, Vol. 49, 2008, Nos. 3–4, pp. 231–254.

[37] Hofer, R. R., Jankovsky, R. S., and Gallimore, A. D., "High-Specific Impulse Hall Thrusters, Part 1: Influence of Current Density and Magnetic Field," *Journal of Propulsion and Power*, Vol. 22, No. 4, 2006, pp. 721–731. doi:10.2514/1.15952

[38] Kim, H., Lim, Y, Choe, W., and Seon, J., "Effect of Multiply Charged Ions on the Performance and Beam Characteristics in Annular and Cylindrical Type Hall Thruster Plasmas," *Applied Physics Letter*, Vol. 105, No. 14, 2014, Paper 144104. doi:10.1063/1.4897948

[39] Kwon, K., Walker, M. L. R., and Mavris, D. M., "Study on Anomalous Electron Diffusion in the Hall Effect Thruster," *International Journal of Aeronautical and Space Sciences*, Vol. 15, No. 3, 2014, pp. 320–334. doi:10.5139/IJASS.2014.15.3.320

[40] Martinez, R. A., and Walker, M. L. R., "Propellant Thermal Management Effect on Neutral Residence Time in Low-Voltage Hall Thrusters," *Journal of Propulsion and Power*, Vol. 29, No. 3, 2013, pp. 528–539. doi:10.2514/1.B34702

[41] Mazouffre, S., Echegut, P., and Dudeck, M., "A Calibrated Infrared Imaging Study on the Steady State Thermal Behaviour of Hall Effect Thrusters," *Plasma Sources Science and Technology*, Vol. 16, No. 1, 2007, pp. 13–22. doi:10.1088/0963-0252/16/1/003

[42] Ito, T., Gascon, N., Crawford, W. S., and Cappelli, M. A., "Experimental Characterization of a Micro-Hall Thruster," *Journal of Propulsion and Power*, Vol. 23, No. 5, 2007, pp. 1068–1074. doi:10.2514/1.27140

[43] Ding, Y., Boyang, J., Sun, H., Wei, L., Peng, W., Li, P., and Yu, D., "Effect of Matching Between the Magnetic Field and Channel Length on the Performance of Low Sputtering Hall Thrusters," *Advances in Space Research*, Vol. 61, No. 3, 2018, pp. 837–843. doi:10.1016/j.asr.2017.11.003

[44] Kim, E., Lee, H., and Kim, E. D., "Sub-Half Meter Imaging Satellite, SpeceEye-X," *Proceedings of 8th International Conference on Recent Advances in Space Technologies*, IEEE, New York, 2017, pp. 125–127. doi:10.1109/RAST.2017.8002971

[45] Frieman, J. D., Liu, T. M., and Walker, M. L. R., "Background Flow Model of Hall Thruster Neutral Ingestion," *Journal of Propulsion and Power*, Vol. 33, No. 5, 2017, pp. 1087–1101. doi:10.2514/1.B36269

J. Blandino
Associate Editor